ELSEVIER

Journal of Hazardous Materials B137 (2006) 856–864

Journal of Hazardous Materials

www.elsevier.com/locate/jhazmat

Oxidation of pesticides by in situ electrogenerated hydrogen peroxide: Study for the degradation of 2,4-dichlorophenoxyacetic acid

Carla Badellino, Christiane Arruda Rodrigues, Rodnei Bertazzoli *

Faculty of Mechanical Engineering, Department of Materials Engineering, State University of Campinas, CP 6122, 13083-970 Campinas, Sao Paulo, Brazil

Received 23 January 2006; received in revised form 2 March 2006; accepted 3 March 2006
Available online 16 May 2006

Abstract

This paper reports an investigation on the performance of the H_2O_2 electrogeneration process on a rotating RVC cylinder cathode, and the optimization of the O_2 reduction rate relative to cell potential. A study for the simultaneous oxidation of the herbicide 2,4-dichlorophenoxyacetic acid (2,4-D) by the in situ electrogenerated H_2O_2 is also reported. Experiments were performed in 0.3 M of K_2SO_4, pH of 10 and 3.5. Oxygen concentration in solution was kept in 25 mg L^{-1}. Maximum hydrogen peroxide generation rate was reached at −1.6 V versus SCE for both, acidic and alkaline solutions. Then, 100 mg L^{-1} of 2,4-D was added to the solution. First order apparent rate constants for 2,4-D degradation ranged from 0.9 to 6.3 × 10^{-5} m s^{-1}, depending on the catalyst used (UV or UV + Fe(II)). TOC reduction was favored in acidic medium where a decreasing of 69% of the initial concentration was observed in the process catalyzed by UV + Fe(II). This figure was an indication that some of the intermediates derived from 2,4-D decomposition remained in solution, mainly as lighter aliphatic compounds.

Keywords: Hydrogen peroxide; Hydrogen peroxide electrosynthesis; Photo-Fenton; Oxygen reduction; 2,4-Dichlorophenoxyacetic acid (2,4-D); AOP

1. Introduction

The use of hydrogen peroxide may offer an efficient means of controlling pollution in aqueous media. Hydrogen peroxide is still one of the most popular non-selective oxidizing agent used for the oxidation of organic pollutants to carbon dioxide. Its reactivity is determined largely by the ratio of the concentration of H_2O_2 to substrate and reaction conditions, particularly in the presence of Fe ions and UV radiation that catalyses hydroxyl radicals formation. Furthermore, hydrogen peroxide reactions leave no residuals in the reaction stream. When used in dilute solutions such as those produced in electrolysis cells, its reactions are non-hazardous and carried out in moderate conditions. In the recent past, several papers have demonstrated that in situ electrogenerated H_2O_2 may also be used successfully for effluent treatment [1–10]. H_2O_2 electrosynthesis is also of interest because of the cost and hazards associated with the transport, storing and handling of concentrated hydrogen peroxide. Graphite flat plates [1,2] and three-dimensional electrodes, made from reticulated vitreous carbon (RVC) [3–5] and gas diffusion electrodes [6–12] have been used to reduce oxygen to hydrogen peroxide at rates which are appropriate to the needs of effluent treatment, in mild conditions of current density and solution pH.

This paper reports an investigation on the performance of the H_2O_2 electrogeneration process on a rotating RVC cylinder cathode, and the optimization of the O_2 reduction rate relative to cell potential. Furthermore, a study for the simultaneous oxidation of the herbicide 2,4-dichlorophenoxyacetic acid (2,4-D) by the in situ electrogenerated H_2O_2 is also reported.

The 2,4-D is an aryloxoalkanoic acid that works as a systemic herbicide being used to control many types of broadleaf weeds. Human exposure occurs through agricultural use, food products, or through lawn and garden use. Continuous use may cause soil percolation and groundwater contamination. Effects of exposure of professional applicators, homeowners and bystanders have been studied, but the risk of 2,4-D to human health has not been completely assessed [13]. However, the central nervous system is a target organ for the effects of this herbicide in different animal species [14].

* Corresponding author. Tel.: +55 19 37883311; fax: +55 19 37883311.
E-mail address: rbertazzoli@fem.unicamp.br (R. Bertazzoli).

0304-3894/$ – see front matter © 2006 Elsevier B.V. All rights reserved.
doi:10.1016/j.jhazmat.2006.03.035

Due to the 2,4-D's refractoriness to degradation, an increasing interest in the use of alternative processes for the pesticide oxidation has been registered in the literature. Advanced oxidation processes using titanium dioxide [15] and zinc oxide [16] as photo catalysts have been reported and the yield of 2,4-D degradation has shown to be dependent on the mass of semiconductor, temperature and solution pH. Nevertheless, the measured TOC values remained constant during illumination, which indicates that mineralization hardly occurs. Ozonation, when catalyzed with UV light in the presence of iron ions, has presented high efficiency for the degradation of 2,4-D, its aromatic intermediates and organic acids. Hydrogen peroxide and Fenton reagent, both catalyzed by UV radiation, also have shown higher conversion rates to carbon dioxide [17–19].

Considering the challenge represented by the refractoriness of 2,4-D to degradation by the attack of hydroxyl radicals [20,21], it was chosen to evaluate the performance of the in situ electrosynthesis of hydrogen peroxide process and the simultaneous oxidation of an organic pollutant. Kinetics of degradation and the route of 2,4-D fragmentation will be also investigated.

2. Experimental details

2.1. Apparatus

Fig. 1 shows the RVC rotating cylinder electrode used for the experiments, with a screw adaptable to the PAR 616 RDE module. The 35 mm long cylinder (diameter of 11 mm) was shaped from a 60 ppi RVC plate. This material presents an average specific area of 3900 $m^2\,m^{-3}$, according to the manufacturer's literature. The RVC cylinder was bonded to the brass screw using the thermally curable Dylon PX Grade Graphpoxy conducting epoxy. When necessary, a vitreous carbon rotating disc electrode ($A = 0.12\,cm^2$) was also used. All experiments were controlled by an Autolab PGSTAT 30 potentiostat/galvanostat. The experiments were run in a 100 mL three electrode cell, with a water jacket to keep temperature in the range from 8 to 10 °C. A platinum foil was used as counter electrode with an area large enough to cover the inner perimeter of the electrochemical cell, such that the RVC working electrode was completely surrounded by the counter electrode. A saturated calomel electrode (SCE) was used as reference. In the experiments in which H_2O_2 oxidizing action was catalyzed by UV radiation, an 8 W Sankyo Denki G8T5 (fluency rate of 31.1 $J\,m^2\,s^{-1}$ and $\lambda_{max} = 254$ nm) germicidal lamp was inserted into the electrochemical cell.

Fig. 1. 60 ppi RVC rotating cylinder cathode.

2.2. Solutions

Supporting electrolyte was always K_2SO_4 0.3 M and NaOH or H_2SO_4 were added to pH of 10 or 3.5, respectively. For the electrolysis carried out in acidic medium, pH dropped from 3.5 to 2.5 at the first moments of the electrolysis and then became constant. Oxygen was thoroughly bubbled into the solution to keep a 25 $mg\,L^{-1}$ concentration of dissolved oxygen, monitored by an Orion DO sensor. Analytical grade Aldrich 2,4-D was used as received and 100 $mg\,L^{-1}$ was added to the supporting electrolyte for the experiments. After 2,4-D addition, solution presented TOC value of around 50 $mg\,L^{-1}$. When need, 1 mM of $FeSO_4$ was added to the solution. Volume of solution used for all experiments was 130 mL.

2.3. Analytical control

Hydrogen peroxide concentration was determined by potentiometric titration using a standardized $KMnO_4$ 0.01N solution in an automatic 702SM Metrohm titrator. 2,4-D degradation was followed by a Shimadzu HPLC equipment, with a Supelco LC-18 reversal phase column, 5 μm × 4.6 mm × 250 mm, and $H_2O/CH_3CN/CH_3COOH$, 52:46:2 (%/%/%) mobile phase. UV detector was set at 280 nm and the flow rate was 1.2 $mL\,min^{-1}$. Formation and degradation of 2,4-D intermediates were also followed by HPLC. Analytical grade 2,4-D (Aldrich) was used to establish a calibration curve in a concentration range from 0 to 100 $mg\,L^{-1}$ for 2,4-D. Similar calibration curves were obtained in the concentration range from 0 to 50 $mg\,L^{-1}$ for the intermediates which are 2,4-dichlorophenol (2,4-DCP), 2,4-dichlororesorcinol (2,4-DCR), 4,6-dichlororesorcinol (4,6-DCR), 2-chlorohydroquinone (2-CHQ) and 2-chlorobenzoquinone (2-CBQ), all purchased from Aldrich.

The main aromatic intermediates, resulting from the oxidation of 2,4-D, were identified by an 5988A HP GC-MS. One-millilitre samples were adjusted with HCl 50% and extracted from the aqueous phase with ethyl acetate. The organic phase was then analysed in the GC–MS equipment. An polyethyleneglycol Inovax column was used and temperature program was 5 min at 35, 35–150 °C at 20 °C/min, 2 min at 150 °C and 150–250 °C at 30 °C/min, then kept by 3 min.

Total organic carbon (TOC) values were obtained in a TOC 5000 Shimadzu equipment. Chemical oxygen demand (COD) was measured using a Hach 45600 closed reflux digester and a Hach DR/2010 spectrophotometer.

2.4. Procedures

Experiments reported here are basically conducted at constant potential. Controlled potential electrolysis was used for the

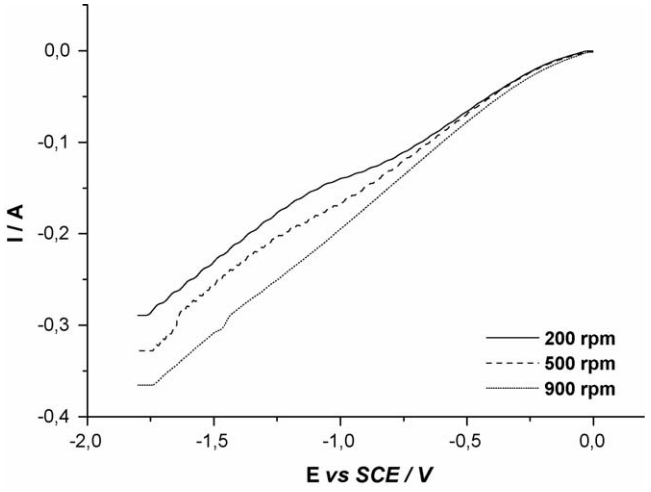

Fig. 2. *I*/*E* response for O_2 reduction reaction on RVC cathode for the rotation rates as shown. Potential scan rate of 100 mV s^{-1}, from 0.0 to −1.8 V, in a 0.3 M K_2SO_4, pH 10, oxygen saturated solution.

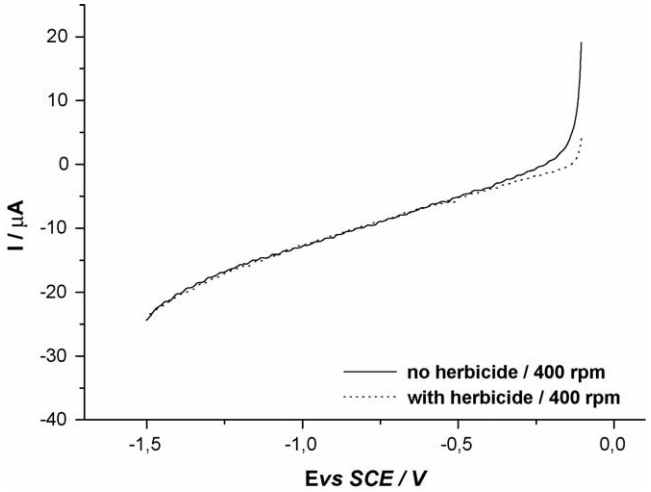

Fig. 3. Fifth cycle voltammogram for solutions nitrogen purged with and without 2,4-D. Potential scanned at 50 mV s^{-1}, from −0.1 to −1.5 V vs. SCE. Solution composition as in Fig. 2.

optimization of H_2O_2 electrogeneration rate related to potential and temperature. During electrolysis of O_2 saturated solutions, catholyte was sampled at pre-determined time intervals and H_2O_2 concentration was measured. Then, a H_2O_2 electrogeneration rate was obtained as a function of potential within the range from −0.5 to −1.9 V versus SCE. Another tool for assessing the range of potential in which H_2O_2 is generated at suitable rates is the linear sweep voltammetry. However, current response of foam type electrodes does not allow a clear identification of mass transfer limited electrochemical reactions [22]. Ohmic losses within the porous electrode may change a mass transfer limited regime to a mixed controlled process, where electron transfer plays a role. Thus, limiting current penetration depth into the cathode material may be limited to less than 2 mL, and current density drops steeply towards the inner portions of the electrode [23]. Fig. 2 shows the *I*/*E* response for a potential scan from 0.0 to −1.8 V in a 0.3 M K_2SO_4, pH 10, oxygen saturated solution, at a scan rate of 100 mV s^{-1}. As limiting current plateaus are not defined on the three-dimensional electrode the choice of a working potential, in which the reaction is fully mass transfer controlled, is not possible. Then, a range of potential must be chosen for the optimization of H_2O_2 electrosynthesis rate. Once the process was optimized, the pesticide was added to the supporting electrolyte and its degradation was followed by HPLC.

3. Results and discussion

3.1. Electrochemical reduction of 2,4-D

As the in situ generation of hydrogen peroxide is an electrochemical reduction process, it was necessary to certify that 2,4-D do not undergo itself to degradation by a reduction reaction. Then, cyclic voltammetry was used for the identification of possible reduction reactions. Potential was scanned from −0.1 to −1.5 V versus SCE, at 50 mV s^{-1}, on a vitreous carbon disc electrode surface. Data recorded for a nitrogen purged supporting electrolyte were compared to those recorded for the same solution in which 2,4-D was added. Fig. 3 shows the fifth cycle voltammograms comparison, in which current response are superimposed. The presence of the 2,4-D in solution do not modifies the response of the supporting electrolyte. Current response of some tens of microamps are due to discharge of water adsorptive and desorptive processes. Data depicted in Fig. 3 resulted from the pH 10 alkaline solution. Even considering that the potentials are slightly

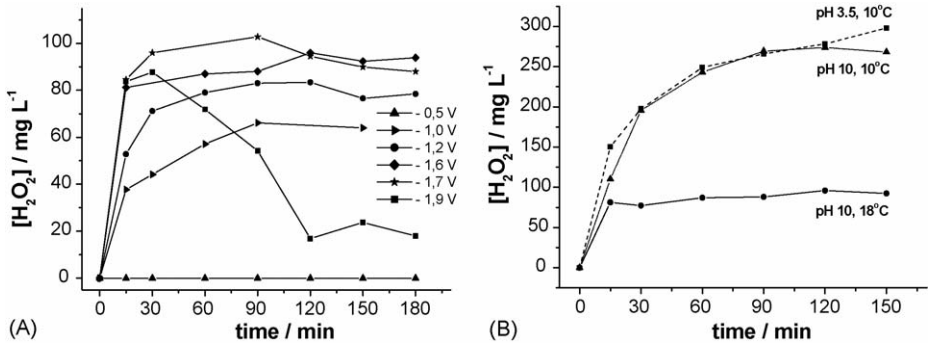

Fig. 4. H_2O_2 concentration as a function of electrolysis time. (A) Concentration profiles for the applied potentials as shown. (B) Concentration profiles for temperatures and pH as shown. Solution of K_2SO_4 0.3 M.

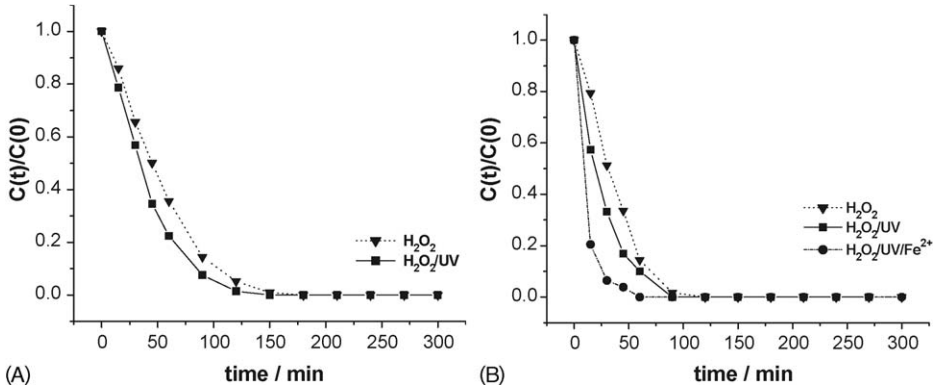

Fig. 5. 2,4-D normalized concentration decay as a function of electrolysis time for the process as indicated. (A) pH 10 solution. (B) pH 3.5 solution.

shifted more positive for the pH 3.5 solution, no signs of 2,4-D reduction were found during similar experiment in acidic medium.

3.2. Hydrogen peroxide electrogeneration

Experiments for the optimization of the generation rate of hydrogen peroxide in alkaline medium were conducted using a 0.3 M K_2SO_4, pH 10 solution, in which O_2 concentration was kept in 25 mg L^{-1}. Potential was ranged from −0.5 to −1.9 V and the RVC electrode was rotated at 900 rpm, limiting value for vortex formation on the solution surface. Fig. 4a shows curves of hydrogen peroxide concentration as a function of electrolysis time obtained at a temperature of 18 °C. Until the potential value of −1.7 V, H_2O_2 concentration increased steeply at the beginning of the electrolysis showing a tendency for stabilization. Final concentration value increased with potential until −1.7 V. From this potential value, the rate of hydrogen peroxide generation decreased as potential increased and higher overpotential values favored water formation, or the reduction of O_2 direct to H_2O, in a four electrons exchanged reaction. As a result, H_2O_2 concentration do not stabilizes, as can be seen for the potential of −1.9 V. Temperature also plays an important role in the electrosynthesis of hydrogen peroxide. Fig. 4b shows that by reducing temperature to 10 °C, final concentration of hydrogen peroxide was three times higher at the potential of −1.6 V. This is due to an increasing of oxygen solubility in the solution and also to a greater stabilization of the hydrogen peroxide as a consequence of a decreasing in the competing decomposition rate. Fig. 4b also shows that, by changing solution pH from 10 to 3.5, there is no appreciable gain in the reaction rate. Considering the results reported here, the experiments for the degradation of 2,4-D were conducted at −1.6 V and 10 °C.

3.3. Experiments of 2,4-D degradation

In a new series of experiments for 2,4-D degradation, electrolysis was conducted in the potential of −1.6 V, at temperature of 10 °C. An amount of 100 mg L^{-1} of the pesticide were then added to the 0.3 M K_2SO_4 supporting electrolyte. Fig. 5A and B shows profiles of the pesticide normalized concentration decay in the alkaline medium and acidic medium, respectively. In the absence of any catalyst, 2,4-D degradation rate is favored in acidic solution. Hydrogen peroxide ability for oxidizing an organic substrate (R) in alkaline and acidic media is due to the reactions below

$$HO_2^- + H^+ + R \rightarrow RO + H_2O \quad (1)$$

$$H_2O_2 + R \rightarrow RO + H_2O \quad (2)$$

However, when catalyzed by UV radiation, hydrogen peroxide decomposes into hydroxyl radicals ($OH^\bullet$), according to

$$H_2O_2 \xrightarrow{h\nu} 2\,OH^\bullet \quad (2')$$

Thus, hydroxyl radicals are responsible by the combustion of the organic compound as follows:

$$R + OH^\bullet \rightarrow CO_2 + H^+ + e^- \quad (3)$$

The synergic effect of both processes (reactions (1) and (3)) may be observed by the higher 2,4-D UV degradation rate in Fig. 5A and B, and higher rate of decomposition was observed when the process was UV assisted (H_2O_2/UV process). On the other hand, acidic medium is still favoring the pesticide degradation. By comparing curves of pesticide concentration decay from Fig. 5A and B, it is possible to note that degradation rate is always higher in solution with initial pH of 3.5. Even considering that, solution pH do not interfere in the H_2O_2 electrogeneration rate, the acidic medium favored the 2,4-D hydroxylation reaction. Fig. 5B also compares the action of H_2O_2 on the pesticide for the H_2O_2/UV process and for the H_2O_2/UV/Fe(II) process (photo-electro-Fenton process). The last dropped the 2,4-D concentration to a value close to zero in less than the half of the time need for the other processes. The outstanding performance is also due to an increasing in the H_2O_2 decomposition rate to $OH^\bullet$ catalyzed by Fe(II) ions in solution according to

$$Fe^{2+} + H_2O_2 \rightarrow Fe^{3+} + OH^- + OH^\bullet \quad (3')$$

Then, Fe(III) is reduced to Fe(II) by both, electron transfer at the cathode surface and photo-reduction, thus regenerating Fenton's reagent according to

$$Fe^{3+} + e^- \rightarrow Fe^{2+} \quad (4)$$

$$[Fe(OH)]^{2+} + h\nu \rightarrow Fe^{2+} + OH^\bullet \quad (5)$$

Table 1
Electrolysis times for the removal of 90% of 2,4-D concentration and for the processes as shown, and apparent rate constants (k) for the degradation

	pH 10		pH 3.5		
	H_2O_2	H_2O_2/UV	H_2O_2	H_2O_2/UV	H_2O_2/UV/Fe(II)
$t_{90\%}$ (min)	100	85	75	62	25
$k \times 10^{-5}$ m s^{-1}	0.9 (R = 0.992)	1.3 (R = 0.991)	1.3 (R = 0.992)	2.1 (R = 0.999)	6.3 (R = 0.996)

Table 1 shows a general comparison between electrolysis times demanded for the removal of 90% of 2,4-D initial concentration according to the processes selected for the experiments.

3.4. Evolution of 2,4-D intermediates concentration

The pesticide intermediates derived from the oxidation processes were followed by HPLC. Samples taken from the process of 2,4-D degradation by non-catalyzed H_2O_2 solution at pH 10 was firstly examined. Fig. 6 (A–C) shows some of the chromatograms obtained during the electrolysis time. Fig. 6(D) also shows the simultaneous evolution of the 2,4-D derivatives normalized concentration. Peak 1 (retention time of 7 min), that decreases rapidly, is related to 2,4-D and the peak 2, at 8.3 min is a result of the first attack by hydroxyl radicals in which 2,4-dichlorophenol (2,4-DCP) is formed. Other hydroxylated derivatives can be observed by peaks 3 (retention time of 5.5 min) and 4 (retention time of 3.9 min) which are 2,4-dichlororesorcinol (2,4-DCR) and 4,6-dichlororesorcinol (4,6-DCR), respectively. Peak 5, at 3 min, represents the early stages of dechlorination and the formation of 2-chlorohydroquinone (2-CHQ). No peak of 2-chlorobenzoquinone (2-CBQ) has been detected as previously reported [20]. As can be seen, the solution remaining from the H_2O_2 non-catalyzed process is still presenting 2,4DCR and 2-CHQ concentrations, and Fig. 6(D) shows that removal of 2-CHQ is less than 90% after 6 h of electrolysis. This is an indication that total mineralization in the non-catalyzed process hardly occurs as we will see later by analyzing TOC results.

Except by the 2-CHQ, all other aromatic derivatives such the dichlorophenol and both dichlororesorcinol were also identified by GC–MS. By expanding the more intensive peaks present in the total ions chromatogram of the sample taken at 60 min of electrolysis, the compounds above were identified by their fragmentation mechanism.

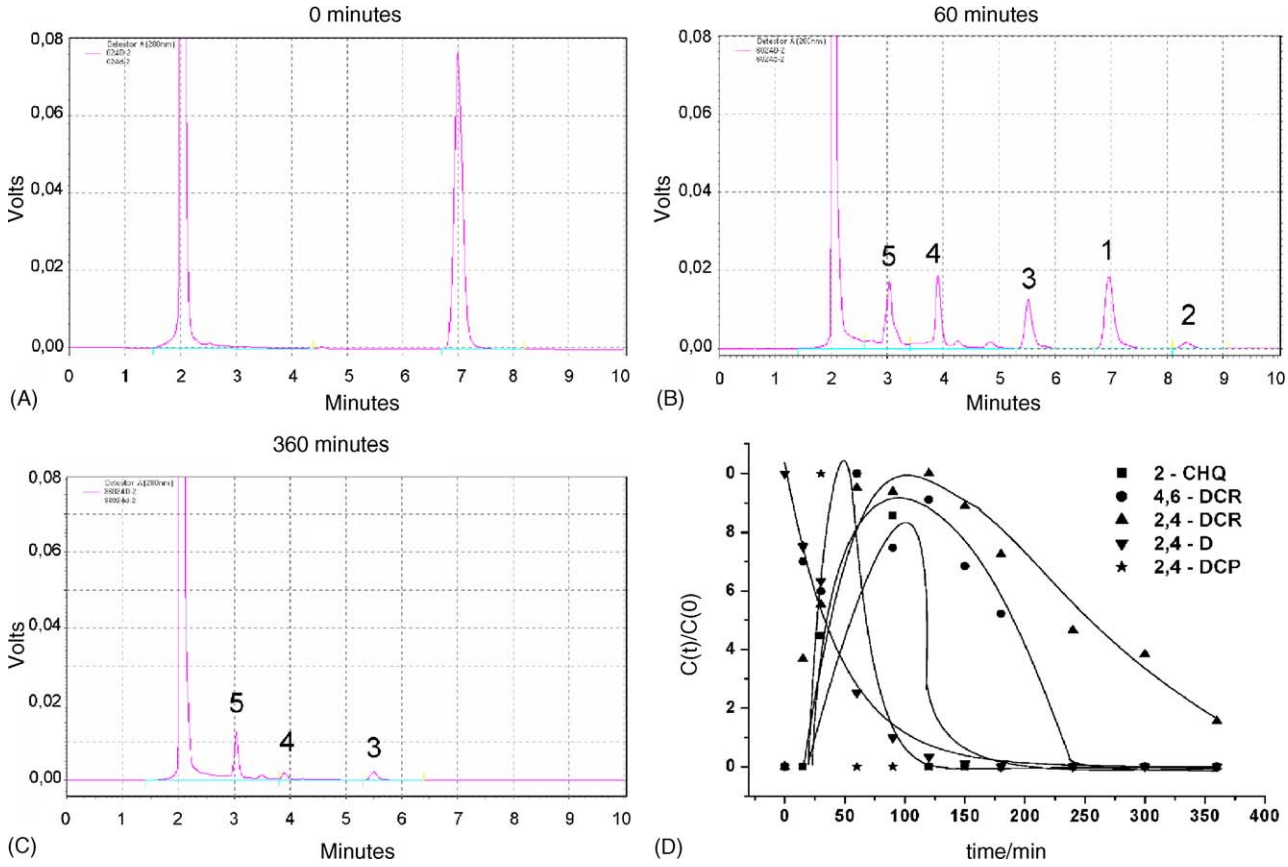

Fig. 6. HPLC chromatograms for the samples taken at (A) 0 min, (B) 60 min and (C) 360 min. (D) Concentration evolution of 2,4-D and its derivatives with electrolysis time. Process of H_2O_2 electrogeneration, at pH 10, without catalysts.

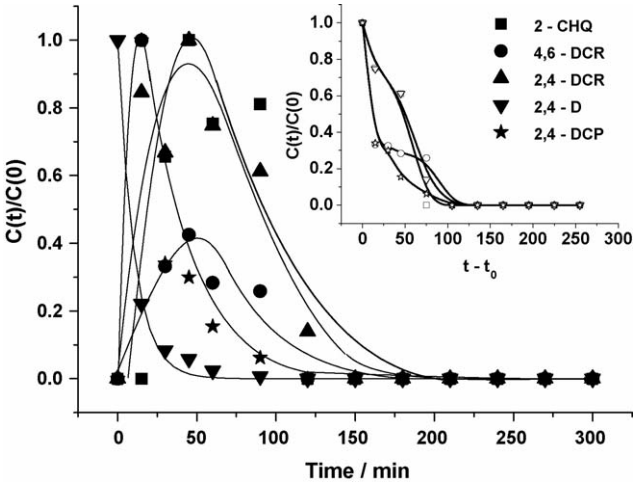

Fig. 7. Concentration evolution of 2,4-D and its derivatives with electrolysis time. Inset: derivatives concentration as a function of time ($t - t_0$) where t_0 is the inflexion points of each curve. H_2O_2 + UV + Fe(II) process, at pH 3.5.

In a new series of experiments, the samples obtained from the photo-electro-Fenton (H_2O_2 + UV + Fe(II)) process were also followed by HPLC. Chromatograms show the same peaks pointing out to the formation of the same intermediates, however at different rates of formation and degradation. Fig. 7 shows that after 3 h of processing, none of the aromatic 2,4-D by-products remain in solution. The chromatogram of the sample taken at 180 min is reduced to a base line, except of the sulfate peak. By-products concentration increases steeply until the rate of formation becomes equivalent to the rate of decomposition. At this moment of the process, curves of concentration present an inflection point from which the intermediate degradation rate is a mandatory process. Inflection points for 2,4-DCP and 2,4-DCR appears at 15 min of processing and for 4,6-DCR and 2-CHQ at 50 min since they result from the decomposition of 2,4-DCR. Considering these inflection points as t_0 and referring the time of electrolysis to t_0, comparison among intermediates degradation curves shows that the decaying concentrations approaches an exponential decay, as an example of 2,4-D concentration. These behaviors are shown in the inset from Fig. 7. A pseudo-first order kinetic in this kind of process is an indication of the presence of an steady state concentration of hydroxyl radicals resulting from H_2O_2 decomposition, which is much more effective when compared to the non-catalyzed process. As will be discussed later, H_2O_2 concentration remaining in solution during electrolysis is much lower for the catalyzed process, although it is being formed at the rates shown in Fig. 4.

Considering the information collected through the chromatograms and taking into account results reported in the literature [20,21], it is possible to summarize a schematic pathway for the degradation of 2,4-D. Fig. 8 shows the proposed pathway, that includes the formation of 2,4-DCR by attack of hydroxyl radicals to the ring and, in the other arm, the formation of 2,4-DCP by attack to the side chain. The compound 2-CBQ, although not detected by all the analytical means, was included as a natural sequence of transformation of 2-CHQ.

3.5. Kinetics of 2,4-D removal

The effect of UV assistance and Fe(II) addition on the 2,4-D oxidation rate may be better compared by a kinetic analysis of the time dependent concentration decay curves. Exponential decaying profiles from Fig. 5 were used for the calculation of the apparent rate constants for 2,4-D degradation, and Fig. 9 presents the plot of $\ln [C(t)/C(0)]$ versus time. Straight lines obtained in these plots are the confirmation of a pseudo-first order 2,4-D concentration decay during the treatment. This linear relationship results from the solution of the mass balance differential equation, and may be written as

$$C(t) = C(0) \exp - \left(\frac{Ak}{V}\right) t \quad (6)$$

where $C(0)$ is the initial 2,4-D concentration, A the active electrode area, V the volume of the solution being processed, t treatment time and k is the apparent rate constant for 2,4-D oxidation, which may be calculated from the slope in the plot of $\ln [C(t)/C(0)]$ versus t. For a porous electrode, active area (A) is represented by the product $A_e V_e$, where A_e is the specific area and V_e is the electrode volume. Considering the electrode dimensions described earlier and a current penetration depth of 1.5 mm usually observed for electrolysis on porous materials [23], active electrode area during the experiments was 32 cm^2. Then, slopes from Fig. 9 were used for apparent rate constants calculations for the different oxidative processes. Table 1 also shows k values followed by their respective fitting coefficients (R). Apparent rate constants for 2,4-D degradation are comparable to the ones observed for electrolysis of solutions containing free cyanide [24] and phenol [25] on TiO_2–RuO_2 oxide anodes. Furthermore, k values for 2,4-D hydroxylation are of the same order of magnitude of those obtained in photo-assisted electrolysis of E1 Kraft mill effluent from the first alkaline extraction of lignin in pulp and paper manufacturing [26]. This is an indication of the applicability of this process as an alternative to conventional treatments as electrolysis on oxide anodes has been.

3.6. H_2O_2 remaining concentration during 2,4-D oxidation

During the removal of 2,4-D from solution, H_2O_2 still being generated and consumed. However, H_2O_2 remaining concentration as a function of the electrolysis time presented a different behavior when compared to those from Fig. 4 and, as expected, H_2O_2 is consumed by decomposition to $OH^\bullet$ and oxidation of the substrate. Fig. 10 reproduces, as upper curve, the H_2O_2 concentration profile from Fig. 4a obtained in the absence of the pesticide. Then, Fig. 10 also compares this concentration profile to those measured in the presence of the substrate being oxidized. Increasing concentration values are observed at the beginning of the electrolysis and then, H_2O_2 concentration decreases as a result of the decomposition into hydroxyl radicals and the hydroxylation of 2,4-D. By assisting the process with UV, the rate of H_2O_2 decomposition increases and peak of concentration is lower. As a result, more hydroxyl radicals become available for the pesticide oxidation, which is confirmed by the results depicted in Fig. 5. When Fe(II) ions are added to the solution,

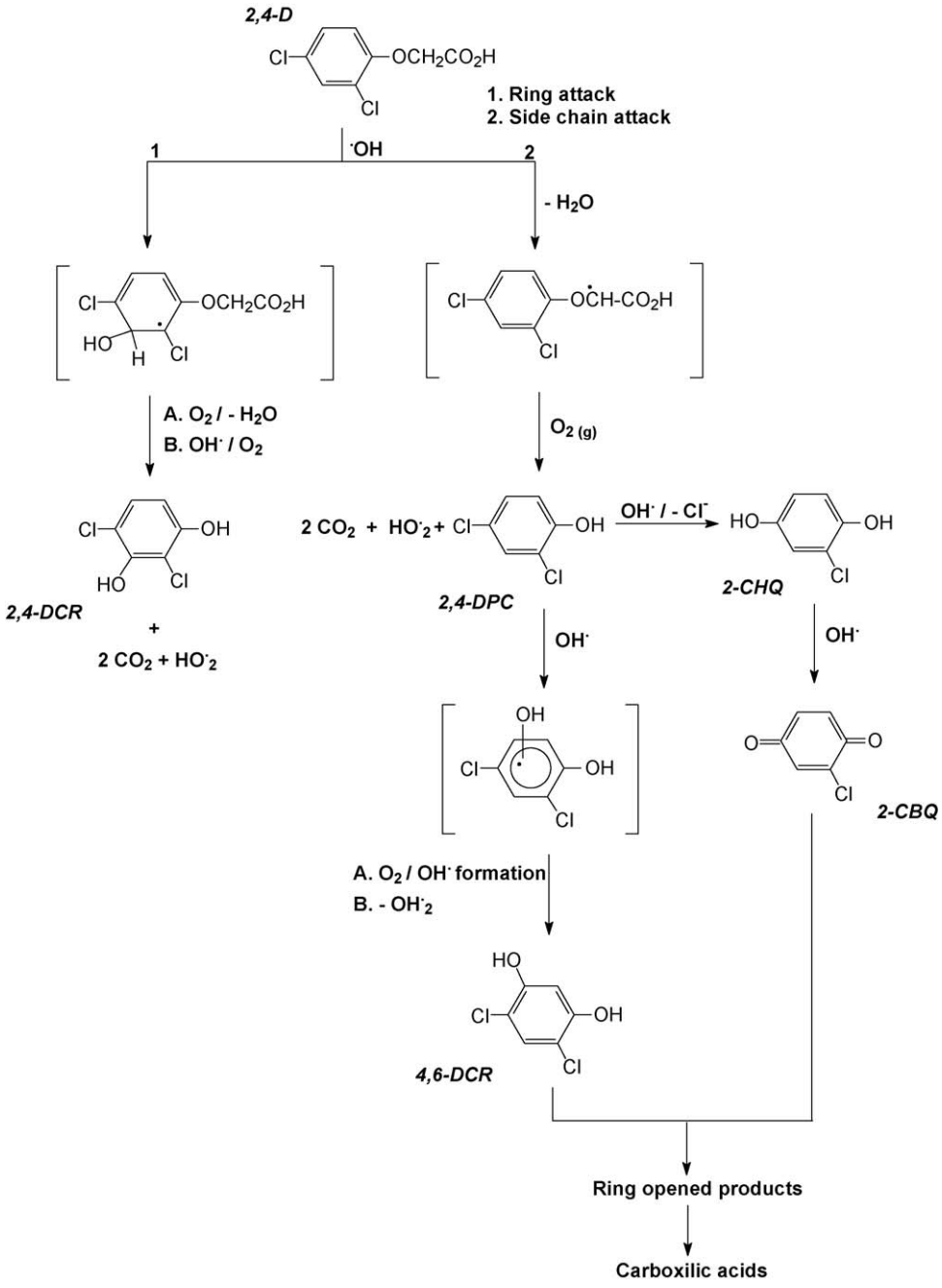

Fig. 8. Summarized pathway for the degradation of 2,4-D.

decomposition of H_2O_2 into hydroxyl radicals is speeded up. Electrogenerated hydrogen peroxide is promptly decomposed according to the reaction represented by Eq. (3), and 2,4-D oxidation rate increases (see Fig. 5b). As a result, Fig. 10 shows that, in the presence of iron, only residuals of H_2O_2 can be measured in the course of the process of 2,4-D oxidation.

3.7. Conversion of 2,4-D to carbon dioxide

Conversion of 2,4-D to carbon dioxide may be followed by TOC concentration. Reduction of TOC concentration is not so expressive in alkaline medium. As shown in Table 2, a reduction of around 20% of TOC was observed at pH 10 even considering the observed decreasing of 90% of 2,4-D concentration. In acidic medium, TOC concentration decay was more expressive, from 57% to 69%, depending on the process considered (see Table 2). In this table an extra experiment appears carried out in acidic medium in which the lamp was not used. For this experiment just TOC initial and final values were measured and 67% of TOC was removed. This an evidence that the role of illumination in Fe(II) presence is secondary and the iron circle, represented by Eqs. (4) and (5), is mandatory in regenerating Fenton's reagent.

As a final consideration, results of TOC reduction, depicted in Table 2, are an indication that some of the intermediates

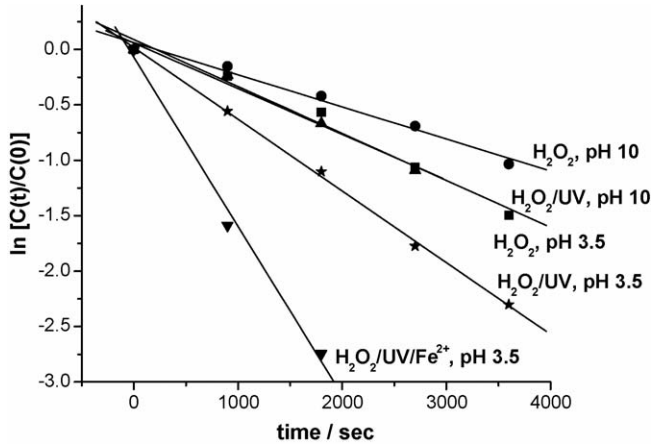

Fig. 9. Linearized 2,4-D normalized concentration decay as a function of electrolysis time for the processes studied. Data taken from Fig. 5.

derived from 2,4-D decomposition remain in solution. However, examination of the intermediates concentration profiles from Fig. 7 shows that the TOC concentration remaining in solution (31%) is probably due to ring opened derivatives and carboxylic acids. Thus, most of the organically bonded carbon concentration remaining in solution is possibly in aliphatic organic compounds form, which may be easily biodegraded.

3.8. Current efficiency and energy consumption

Current efficiency for the generation of hydrogen peroxide is still low and immobilization of organic catalysts on RVC cathode is part of going on studies in our group. Low efficiency in electrosynthesis of hydrogen peroxide is an evidence that most of the dissolved oxygen undergoes a four electrons reaction with water as a final product. At optimized conditions, using potential of −1.6 V versus SCE, cell current and cell potential are 0.18 A and 2.5 V, respectively. In these conditions, 130 mL of a 275 mg L^{-1} solution was generated in a 4 h experiment, at 10 °C

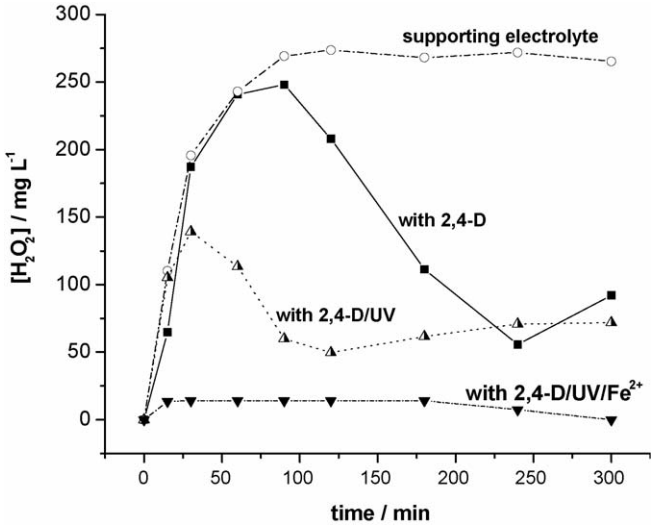

Fig. 10. H_2O_2 concentration remaining in solution during the oxidation of the 2,4-D for the processes as indicated.

Table 2
Percentage of TOC concentration removed (TOC_R) and energy consumed (E_C) per gram of TOC removed for the processes used for 2,4-D degradation

Process	pH 10		PH 3.5	
	TOC_R (%)	E_C (kW h g^{-1})	TOC_R (%)	E_C (kW h g^{-1})
H_2O_2	22	0.16	57	0.06
H_2O_2 + UV	23	2.9	58	1.16
H_2O_2 + Fe(II)	–		67	0.05
H_2O_2 + UV + Fe(II)	–		69	0.98

(please see Fig. 4B). Charged passed was 0.72 A h although only 0.052 A h would be necessary. As a result current efficiency was 7.8% and energy consumption was 0.05 kW h g^{-1} of hydrogen peroxide.

Reduction of TOC concentration is a good parameter for the energy cost estimation of an effluent treatment technology. Energy consumed for TOC degradation in the experiments reported here were 1.8×10^{-3} kW h for the electrolysis and 3.3×10^{-2} kW h for the UV illuminated electrolysis. Taking these values into account, Table 2 also shows the energy consumption for each process showing that photo-electro-Fenton and electro-Fenton processes present an equivalent performance in TOC removal and much less energy is demanded for the electro-Fenton process.

4. Conclusions

Electrogeneration of hydrogen peroxide from oxygen reduction is also an efficient means of controlling organic pollutants concentration in aqueous media. Maximum generation rate was reached at −1.6 V versus SCE for both, acidic and alkaline solutions. Apparent rate constants for 2,4-D degradation ranged from 0.9 to 6.3×10^{-5} m s^{-1}, depending on the catalyst used (UV or UV + Fe(II)).

TOC reduction was favored in acidic medium where 69% of concentration decrease was observed in the H_2O_2/UV/Fe(II) process. Similar performance was reached by the H_2O_2/Fe(II) showing that UV radiation plays a secondary role in Fenton's reagent regeneration. Values for TOC removal are an indication that some of the intermediates derived from 2,4-D decomposition remain in solution. However, by considering the intermediates identified by HPLC and GC–MS and their sequence of degradation, they are lighter aliphatic compounds that, on the contrary of 2,4-D, may be easily biodegraded.

References

[1] J.-S. Do, C.-P. Chen, In situ oxidative degradation of formaldehyde with electrogenerated hydrogen peroxide, J. Electrochem. Soc. 140 (6) (1993) 1632–1637.
[2] J.-S. Do, C.-P. Chen, In situ oxidative degradation of formaldehyde with hydrogen peroxide electrogenerated on the modified graphites, J. Appl. Electrochem. 24 (9) (1994) 936–942.
[3] C.P. De Leon, D. Pletcher, Removal of formaldehyde from aqueous solutions via oxygen reduction using a reticulated vitreous carbon cell, J. Appl. Electrochem. 25 (4) (1995) 307–314.

[4] A. Alvarez-Gallegos, D. Pletcher, The removal of low levels of organics via hydrogen peroxide formed in a reticulated vitreous carbon cathode cell. Part 1. The electrosynthesis of hydrogen peroxide in aqueous acidic solutions, Electrochim. Acta 44 (5) (1998) 853–861.
[5] A. Alvarez-Gallegos, D. Pletcher, The removal of low levels of organics via hydrogen peroxide formed in a reticulated vitreous carbon cathode cell. Part 2. The removal of phenols and related compounds from aqueous effluents, Electrochim. Acta 44 (14) (1999) 2483–2492.
[6] E. Brillas, R.M. Bastida, E. Llosa, J. Casado, Electrochemical destruction of aniline and 4-chloroaniline for waste-water treatment using a carbon-PTFE O_2-fed cathode, J. Electrochem. Soc. 142 (6) (1995) 1733–1741.
[7] E. Brillas, E. Mur, J. Casado, Iron(II) catalysis of the mineralization of aniline using a carbon-PTFE O_2-fed cathode, J. Electrochem. Soc. 143 (3) (1996) L49–L53.
[8] E. Brillas, R. Salueda, J. Casado, Peroxi-coagulation of aniline in acidic medium using an oxygen diffusion cathode, J. Electrochem. Soc. 144 (1997) 2374–2379.
[9] E. Brillas, E. Mur, R. Salueda, L. Sanches, Aniline mineralization by AOP's: anodic oxidation, photocatalysis, electro-Fenton and photoelectro-Fenton processes, Appl. Catal. B: Environ. 16 (1) (1998) 31–42.
[10] T. Harrington, D. Pletcher, The removal of low levels of organics from aqueous solution using Fe(II) and hydrogen peroxide formed in situ at gas diffusion electrodes, J. Electrochem. Soc. 146 (8) (1999) 2983–2989.
[11] E. Brillas, M.A. Banos, S. Camps, C. Arias, P.L. Cabot, J.A. Garrido, R.M. Rodríguez, Catalytic effect of Fe(II), Cu(II) and UVA light on the electrochemical degradation of nitrobenzene using and oxygen-diffusion cathode, New J. Chem. 28 (2) (2004) 314–322.
[12] E. Brillas, P.L. Cabot, R.A. Rodríguez, C. Arias, J.A. Garrido, R. Oliver, Appl. Catal. B: Environ. 51 (2) (2004) 117–127.
[13] S.A. Harris, K.R. Salomon, G.R. Stephenson, Exposure of homeowners, professional applicators and bystanders to 2,4-dichlorophenoxyacetic acid, J. Environ. Sci. Health B: Pestic. Food Contam. Agric. Wastes 27 (1992) 23–38.
[14] A.A. Bortolozzi, A.M.E. Duffard, R. Duffard, M.C. Antonelli, Effects of 2,4-dichlorophenoxyacetic acid exposure on dopamine D_2-like receptors in rat brain, Neurotoxicol. Teratol. 26 (4) (2004) 599–605.
[15] M. Trillas, J. Peral, X. Doménech, Redox photodegradation of 2,4-dichlorophenoxyacetic acid over TiO_2, Appl. Catal. B: Environ. 5 (1995) 377–387.
[16] L. Sanches, J. Peral, X. Doménech, Degradation of 2,4-dichlorophenoxyacetic acid by in situ photogenerated Fenton reagent, Electrochim. Acta 41 (13) (1996) 1981–1985.
[17] J.J. Pignatello, Dark and photoassisted Fe(III) catalyzed degradation of chlorophenoxy herbicides by hydrogen peroxide, Environ. Sci. Technol. 26 (5) (1992) 944–951.
[18] Y.F. Sun, J.J. Pignatello, Chemical treatment of pesticide wastes—evaluation of Fe(III) chelates for catalytic hydrogen peroxide oxidation of 2,4-D at circumneutral pH, J. Agric. Food Chem. 40 (2) (1992) 322–327.
[19] C.Y. Kwan, W. Chu, Photooxidation of 2,4-dichlorophenoxyacetic acid by ferrous oxalate-mediated system, Water Sci. Technol. 49 (4) (2004) 117–122.
[20] E. Brillas, J.C. Calpe, J. Casado, Mineralization of 2,4-D by advanced electrochemical oxidation proceses, Water Res. 34 (8) (2000) 2253–2262.
[21] M.A. Oturan, An ecologically effective water treatment technique using electrochemically generated hydroxyl radicals for in situ destruction of organic pollutants: application to herbicide 2,4-D, J. Appl. Electrochem. 30 (4) (2000) 475–482.
[22] D. Pletcher, I. White, F.C. Walsh, J.P. Millington, Reticulated vitreous carbon cathodes for metal ion removal from process streams. Part I. Mass transport studies, J. Appl. Electrochem. 21 (1991) 659–666.
[23] M.R.V. Lanza, R. Bertazzoli, Removal of Zn(II) from chloride medium using a porous electrode: current penetration within the cathode, J. Appl. Electrochem. 30 (2000) 61–70.
[24] M.R.V. Lanza, R. Bertazzoli, Cyanide oxidation from wastewater in a flow electrochemical reactor, Ind. Eng. Chem. Res. 41 (2002) 22–26.
[25] R.R.L. Pelegrinno, R.A. Di-Iglia, C. Sanches, L.A. Avaca, R. Bertazzoli, Comparative study of commercial oxide electrodes performance in electrochemical degradation of organics in aqueous solutions, J. Braz. Chem. Soc. 13 (1) (2002) 60–65.
[26] R.T. Pelegrini, R.S. Freire, N. Duran, R. Bertazzoli, Photoassisted electrochemical degradation of organic pollutants on a DSA type oxide electrode: process test for a phenol synthetic solution and its application for the E1 bleach Kraft mill effluent, Environ. Sci. Tech. 35 (13) (2001) 2849–2853.